JBC Papers in Press. Published on February 28, 2020 as Manuscript RA119.011842
The latest version is at https://www.jbc.org/cgi/doi/10.1074/jbc.RA119.011842

The Parkinson's disease–associated kinase LRRK2 regulates genes required for cell adhesion, polarization, and chemotaxis in activated murine macrophages

Daniel R. Levy[1], Atul Udgata[1], Panagiotis Tourlomousis[2], Martyn F. Symmons[1], Lee J. Hopkins[2], Clare E. Bryant[2] and Nicholas J. Gay[1*].

From the [1]Department of Biochemistry, University of Cambridge, Tennis Court Road, Cambridge, CB2 1GA, UK; [2] Department of Veterinary Medicine, University of Cambridge, Madingley Road, Cambridge, CB3 0ES, UK

Running title: *Role of LRRK2 in inflammation induced chemotaxis*

[*] To whom correspondence should be addressed: Nicholas J. Gay, Department of Biochemistry, University of Cambridge, Cambridge CB2 1GA, UK; njg11@cam.ac.uk Tel. (+44) 1223 334976.

Keywords: leucine-rich repeat kinase 2 (LRRK2), inflammation, cell adhesion, chemotaxis, Toll-like receptor 4, Parkinson's disease, neurodegeneration, innate immunity, gene expression, transcriptomics

ABSTRACT

Leucine-rich repeat kinase 2 (*LRRK2*) encodes a complex protein that includes both kinase and GTPase domains. Genome-wide association studies have identified dominant *LRRK2* alleles that predispose their carriers to late-onset idiotypic Parkinson's disease (PD) and also to autoimmune disorders such as Crohn's disease. Considerable evidence indicates that PD initiation and progression involve the activation of innate immune functions in microglia, which are brain-resident macrophages. Here, we asked whether LRRK2 modifies inflammatory signaling and how this modification might contribute to PD and Crohn's disease. We used RNA-Seq–based high-resolution transcriptomics to compare gene expression in activated primary macrophages derived from wild-type and *Lrrk2*-knockout mice. Remarkably, expression of a single gene, *Rap guanine nucleotide exchange factor 3* (*Rapgef3*), was strongly up-regulated in the absence of LRRK2 and down-regulated in its presence. We observed a similar regulation of *Rapgef3* expression in cells treated with a highly specific inhibitor of LRRK2 protein kinase activity. *Rapgef3* encodes an exchange protein, activated by cAMP 1 (EPAC-1), a guanine nucleotide exchange factor that activates the small GTPase Rap-1. Rap-1 mediates cell adhesion, polarization, and directional motility, and our results indicate that LRRK2 modulates chemotaxis of microglia and macrophages. Dominant PD-associated *LRRK2* alleles may suppress EPAC-1 activity, further restricting motility and preventing efficient migration of microglia to sites of neuronal damage. Functional analysis *in vivo* in a sub-clinical infection model also indicated that LRRK2 subtly modifies the inflammatory response. These results indicate that LRRK2 modulates the expression of genes involved in murine immune cell chemotaxis.

LRRK2 is a large protein of 286 kDa consisting of a complex and unique arrangement of protein-protein interaction and functional domains. This arrangement consists of N-terminal repeats, including ankyrin repeats, a leucine rich repeat (LRR) domain, a Ras of complex proteins (Roc) GTPase, with associated C-terminal of Roc (COR) domain, a Ser/Thr protein kinase, and finally a WD40 domain at the C-terminus of the protein(1). The presence of a Roc-COR tandem domain defines LRRK2 as a member of the Roco protein family, a family first detected in the slime mould *Dictyostelium discoideum* (2, 3).

There is great interest in all aspects of LRRK2 biology because Genome Wide Association Studies (GWAS) studies have

identified many variants in this protein that predispose to late-onset Parkinson's disease. The most common mutation in the LRRK2 gene results in a change from glycine to serine at amino acid 2019 (G2019S). This SNP is the highest known risk factor for the development of Parkinson's disease, accounting for 5-7 % of autosomal-dominant familial cases (4, 5) and 1-2 % of sporadic cases in western populations (6). GWAS studies have also revealed a link with Crohn's disease and leprosy. Genetic links with these diseases demonstrate a non-neuronal, but clearly innate immune component to LRRK2 biology (7).

LRRK2 expression is enriched in macrophages, B-cells and dendritic cells (8). Innate immune stimuli such as interferon gamma (IFN-γ) stimulate LRRK2 expression, revealing a responsiveness to the activation of innate immune signalling pathways mediated by pattern recognition receptors(9). Furthermore activation of Toll-like receptors (TLRs) by pathogen associated molecules such as bacterial lipopolysaccharide (LPS) leads to phosphorylation of LRRK2 by IκB kinase at two serine residues (Ser 910, Ser935) (10). The IκB kinase family is normally associated with the phosphorylation of IκB proteins that sequester NF-κB in the cytoplasm. Phosphorylation and ubiquitination of IκB proteins leads to proteolysis, and subsequent transfer of NF-κB into the nucleus (11). LRRK2 phosphorylation is dependent on the TLR adaptor (Myd88), an innate immune signal transducer that mediates signalling from cell surface TLRs, as well as TLR7, 8, and 9 which signal from the endosomal compartmen

The role of inflammatory processes in the aetiology of Parkinson's is further illustrated by administration of LPS both systemically and directly into the substantia nigra. In the latter case LPS causes irreversible degeneration of dopaminergic neurons of the pars compacta, observed a week after injection (12, 13). Notably non-dopaminergic neurons of the nigrostriatal system, as well as proximal dopaminergic neurons not associated with the nigrostriatal pathway, remain unaffected by direct LPS injection. Therefore LPS injection and the resulting inflammatory insult demonstrates remarkable sensitivity and specificity to the dopaminergic circuitry associated with Parkinson's disease. Another study demonstrated that the same pattern of Parkinson's disease-like microglial activation, followed by neurodegeneration over ten months was observed when LPS or TNFα were administered systemically in mice via intraperitoneal injection (14). In humans, a laboratory worker accidentally exposed to *Salmonella* derived LPS developed many symptoms of Parkinson's disease including bradykinesia, rigidity and tremor at rest, as well as other neurological problems resulting from damage to the substantia nigra as well as the cerebral cortex (15). Human Parkinsonism has been further linked to immune activation through the role of neurotrophic viral infection, and in particular, infection by the human influenza virus. Individual cases of viral infection leading to neuropathology and death have been reported, as well as increased incidence of Parkinson's disease following pandemic flu, such as experienced in 1918 (16).

At present little is known about how LRRK2 modifies the gene expression programme induced by innate signalling pathways and how this might contribute to Parkinson's disease initiation and progression. In this study we have used high-resolution transcriptomics to compare gene expression in primary macrophages derived from wild-type and LRRK2 deficient mice. This analysis reveals that LRRK2 modulates the expression of a small subset of genes that are involved in chemotaxis and membrane remodelling.

Results

mRNA sequencing, quality control and read mapping

We have used RNA sequencing to determine how LRRK2 modifies gene expression in primary bone marrow derived macrophages from wild type and LRRK2 -/- mice. If valid comparisons are to be made it is necessary to confirm the similarity in nature and purity of macrophage cultures before RNA extraction and RNA sequencing. One day prior to RNA extraction, a portion of differentiated macrophages were prepared for flow cytometry analysis and stained for various cell surface markers: CD11b for cells of the myeloid lineage, F4/80 for mouse macrophages, and CD11c for monocytic-derived cells, including macrophages (17). These markers revealed no significant

differences in the differentiation state of the cells, with uniform expression of CD11b, and highly similar expression levels of F4/80 and CD11c. CD11c surface expression in LRRK2 KO macrophages displayed a slightly higher level of variability between cultures than WT equivalent cells (Fig S1). Overall, cultures were considered similar enough to proceed with differential gene expression analysis.

We then treated WT and LRRK2 -/- macrophages with either LPS or muramyl dipeptide (MDP), activators of the TLR4 and NOD2 mediated innate responses respectively. After two hours of stimulation RNA was extracted for mRNA sequencing. A mean read depth of over $22.2x10^6$ reads/sample was achieved with a range of $16.0x10^6$ - $24.9x10^6$ reads/sample (Table S1). Reads were of high quality, requiring a mean of less than 0.1 % of reads to be trimmed during quality control. A mean of 87.5 % of reads could be unambiguously mapped to gene encoding regions of the genome. Therefore by comparing the frequency of reads per gene between samples, relative levels of expression can be determined. These datasets were then analysed for differential gene expression.

Differential gene expression

Datasets of mapped counts were interrogated for differences in each LRRK2 genotype upon innate immune stimulation, as well as for underlying differences between genotypes in unstimulated cells (Fig 1a). DEseq2 (18) determines a statistical model accounting for variance in counts per gene, and base mean of counts allowing the statistical significance of apparent differences in gene expression to be estimated. This analysis revealed LPS treatment caused differential expression of 4985 and 5354 genes in WT and LRRK2 -/- macrophages respectively. By contrast MDP treatment resulted in 1483 significantly differentially expressed genes in WT macrophages, compared to 1478 genes in LRRK2 KO macrophages (Fig 1b).

In the absence of stimulation only eight genes were significantly differentially expressed (Table 1). One of these is LRRK2 a result that . is confirmed by qPCR. The lesion in the LRRK2 KO mouse deletes part of exon 1 and exon 2 leading to termination at an out of frame stop codon in exon 3. As the LRRK2 transcription unit has 51 exons this should lead to nonsense mediated decay (NMD) of the transcript. The level of transcript measured is about 50% of the wild-type which indicates that NMD is inefficient in this case (19) . Other genes regulated include Kif21a: a member of the kinesin family of motor proteins, Camk2b, a calcium/calmodulin responsive protein kinase, Cd59a: a regulator of the membrane attack complex in mice, and Nnt: a NAD(P) transhydrogenase with implications in defence against oxidative stress. Very little is known about the Lrmda gene except that it consists of a region of LRRs. The remaining results are not represented at the protein level and so are unlikely to have relevance to the current study. The gene detected as being of the highest significance, Gm14150, is described as a pseudogene, produced by the incorporation of reverse transcribed mRNA into the genome, while Gm44305 is a retained intron. These are likely not differentially expressed genes, but pre-existing genomic difference between strains (20).

The broad characteristics of the MDP and LPS responses, as well as similarities and differences between WT and LRRK2 deficient macrophages in their response to innate immune activation were visualised with 'volcano' plots (Fig. 2). In both LPS and MDP experiments, a greater number of genes were up-regulated than down-regulated. LPS treatment led to 3192 genes being up-regulated and 2696 down-regulated, MDP treatment caused 1020 genes to be up-regulated and 676 down-regulated (Fig 1). Furthermore, quantification confirmed that a greater number of genes were differentially expressed upon LPS treatment in LRRK2 deficient macrophages than WT macrophages. Perhaps the most interesting observation from this analysis is that a single gene was found to be down-regulated in wild type macrophages and up-regulated in LRRK2 -/- macrophages upon treatment with LPS. Transcription of this gene, *Rapgef3*, is almost halved upon LPS treatment in WT macrophages while being increased just over 7-fold in LRRK2 null macrophages; a complete reversal in transcriptional regulation upon loss of LRRK2.

Two parameter analysis identifies a small subset of differentially responding genes that are involved in cell motility and chemotaxis

In contrast to conventional differential gene expression analysis, two-parameter analysis provides an alternative method to identify differentially responding genes between genotypes (21) (see http://bioconductor.org/packages/release/bioc/vignettes/edgeR/inst/doc/edgeRUsersGuide.pdf, section3.5). This method revealed eleven genes with significantly different responses to LPS as between wild type and LRRK2 -/- macrophages (Padj < 0.1) (Fig. 3, Table 2). All differentially responding genes showed an increased level of transcription upon LPS stimulation in LRRK2 KO cells compared to WT cells. *Rapgef3* with a Padj value of 5×10^{-37} and a fold change of about 11 was the gene most strongly regulated by the presence of LRRK2. Four other genes identified encode either chemokine ligands (*Ccl3, 4 , 5*) or receptors (*Ccrl2*) that mediate chemotactic responses, suggesting a common theme of regulated motility (see Discussion).

In order to confirm the results of the RNASeq experiments qRT-PCR was used to directly measure the level of 6 of the 11 genes identified in WT and LRRK2 -/- macrophages (Fig. 4A). This confirms the results of the RNASeq analysis for Rapgef3, chemokines and transcription factor Atf-3. We next asked whether chemical inhibition of the LRRK2 kinase also induces the expression of *Rapgef3*. We treated wild-type and LRRK2 -/- macrophages with the highly specific inhibitor GSK2578215A (22). *Rapgef3* was induced about 6 fold in treated, wildtype macrophages as compared to untreated controls. By contrast no differences in expression level were detected when LRRK2 mutant macrophages were treated with GSK2578215A relative to the untreated controls (Fig. 4B). Thus, LRRK2 kinase activity is required for the observed regulation of *Rapgef3* gene expression, consistent with the results of the RNASeq analysis.

In contrast to LPS, MDP treatment identified no significant differentially responding genes (Fig. 3c,d). This aligns with the less immunogenic nature of MDP compared to LPS stimulation and demonstrates the high stringency of the two-parameter method.

Elevated levels of EPAC-1 protein in activated macrophages lacking LRRK2.

To determine whether of *Rapgef3* mRNA and EPAC-1 protein levels are correlated we stained LRRK2 deficient and wildtype macrophages with a fluorescent monoclonal antibody specific for EPAC-1. As shown in Fig. 5a EPAC-1 is ubiquitous and in many cells is distributed in the expected punctate, peri-nuclear pattern (Fig. S2). We then quantified protein levels and 6 hours after treatment with LPS the LRRK2 deficient cells have significantly higher levels of EPAC-1, consistent with the RNASeq and qPCR results (Fig. 5b). We were unable further validate these observations using western blot as the available antibodies are insufficiently specific or sensitive in this assay.

A sustained inflammatory response in LRRK2 knock out mice.

To explore whether LRRK2 affects innate immune function we have used a model of sub-clinical bacterial infection. Wild type and LRRK2 deficient mice were infected with *Salmonella typhimurium* and three markers of inflammation, interleukin 18 (IL-18), interferon γ (IFNγ) and splenomegaly were measured. As shown in Fig. 6 LRRK2 -/- mice have elevated levels of both IL-18 and IFNγ compared to controls at 14 days post challenge. These results are statistically significant ($p < 0.05$, with the exception IFNγ at 14 days $p=0.06$; see legend to Fig 6). This indicates that the absence of LRRK2 causes an enhanced inflammatory response.

Discussion

In this study we investigated how LRRK2 modifies inflammatory signalling mediated by LPS and MDP. We have identified a small subset of genes that are activated by LPS in macrophages that lack LRRK2 but not in wild-type control cells. About half of these molecules are involved in cell migration, motility and chemotaxis. Of particular note is the guanine nucleotide exchange factor (GEF) *Rapgef3*, by far the most strongly induced gene identified with an 11-15 fold increase in transcription in the absence of LRRK2. *Rapgef3* is also the only gene that is down regulated in wild type macrophages but up regulated in LRRK2 -/- cells, as compared to unstimulated control cells. *Rapgef 3* is also derepressed by treatment of macrophages with the highly specific kinase inhibitor

GSK2578215A (22), indicating that inter- or intra- molecular phosphorylation is required.

Rapgef3 encodes EPAC-1 a GEF that mediates cAMP dependent activation of the small G-protein Rap1. EPAC promotes Rap-1 GDP-GTP exchange leading to cell adhesion, cell polarization and enhanced leucocyte chemotaxis (23, 24). On the other hand another study found that LPS treatment paralyzes monocyte chemotaxis, an effect that requires activated Rap-1 (25). It is thus likely that LRRK2 indirectly regulates the mobility of macrophages and microglia that have been activated by innate stimuli such as LPS. An attractive hypothesis is that dominant PD associated LRRK2 alleles such as G2019S that have higher constitutive kinase activity may regulate the motility of macrophages by further suppressing EPAC-1 levels. In that regard a recent study found that G2019S microglia and LRRK2 -/- cells when activated by ADP have retarded and enhanced motility respectively as compared to wild-type control cells. G2019S microglia also have an impaired ability to isolate brain injury (26). These authors present evidence for the involvement of focal adhesion kinases, however this may be indirect and a possible role of the LRRK2/EPAC-1/Rap1 axis should be investigated.

LRRK2 is part of an ancient and highly conserved pathway of directional motility (2). In the slime mould *Dictyostelium gbpC* is one of eleven paralogues of LRRK2. *GbpC* null cells are severely defective in chemotaxis because they cannot polarize cells effectively and have altered patterns of myosin phosphorylation that are probably mediated by activation of Rap1. It is interesting to note also that in *Dictyostelium* many LRRK2 paralogues encode GEFs within their modular structure.

As well as EPAC1 four other messages that function in chemotaxis are differentially expressed. Three are chemokines, and one is a chemokine receptor-like protein. CCL3 and CCL4 are also known as ‘macrophage inflammatory protein 1’; MIP-1α and MIP-1β respectively. CCL5 is also known as ‘regulated on activation, normal T cell expressed and secreted’ (RANTES). These chemokines are all members of the ‘CC Chemokine/Receptor family’ and share a common receptor in CCR5. CCL3 and CCL5 may also bind CCR1, while CCL5 binds a further receptor, CCR3(27). These chemokines are all classified as pro-inflammatory, meaning they are induced by inflammatory stimuli to recruit inflammatory cells to a site of inflammation, as opposed to homeostatic chemokines, which are constitutively expressed in certain tissues (28). CCRL2 is chemokine receptor-like protein, with over 40 % sequence identity to CCR1, CCR2, CCR3 and CCR5 (29) and highest amino acid sequence similarity to CCR1. Interestingly, CCRL2 has been reported as a non-canonical receptor for CCL5 (30), as well as CCL19 and chemerin (31). A microarray screen of unstimulated mouse microglia has shown that CX3CR1, a non-canonical chemokine receptor of fractalkine, expressed exclusively in microglia, is upregulated by knockout of LRRK2 (32). This reaffirms that chemokine responses may be involved in LRRK2 biology in diverse immunological contexts.

Message encoding the transcription factor ATF3 is induced by 3 fold in the absence of LRRK2 and is a negative regulator of pro-inflammatory TLR4 signalling, a part of the LPS induced negative-feedback loop (33, 34). Thus it is possible that G2019S mutation of LRRK2 might down regulate ATF3, resulting in attenuated negative feedback of TLR4 signalling, enhanced inflammation, and greater neuronal stress. Other transcription factors messages identified encode MXD1 and CSRNP1. MXD1 acts in a network with MYC and MAX, forming the MYC/MAX/MXD1 axis (33). MXD1 is in competition with MYC for the binding of MAX leading to a mixture of MXD1/MAX and MYC/MAX dimers controlling transcriptional output. In the context of cancer, MYC signalling affects cell adhesion, cell shape, and reduces cell migration through modulation of the actin cytoskeleton (35). Finally, CSRNP1 is a transcription factor that is upregulated by Axin, as well as inflammatory stimuli in the form of IL-2 (36, 37). Axin is a negative regulator of the Wnt signalling pathway, acting to sequester the transcription factor β-catenin to the cytoplasm (38).

Two transcripts identified have been linked directly to Parkinson’s disease. Abtb2 encodes ‘Ankyrin-rich BTB/POZ domain containing protein-2’ (BPOZ-2). This protein causes inhibition of alpha-synuclein aggregation (39). Lentiviral delivery of the BPOZ-2 gene

appears to stimulate autophagic clearance of alpha-synuclein, resulting in reduced alpha-synuclein pathology in the basal ganglia. Another protein identified is the G protein-coupled receptor, HCAR2, otherwise known as 'niacin receptor 1'. Niacin has been proposed as a treatment for Parkinson's disease, although evidence of efficacy is lacking (40, 41). Activation of HCAR2 in macrophages has an anti-inflammatory effect. Activation by niacin results in inhibition of CCL2 induced macrophage migration (42), as well as an inhibited response to LPS stimulation (43) or inflammatory cytokine release (44).

Previous studies of LRRK2 using kinase inhibitors have revealed immunological functions. However these results should be treated with caution owing to significant off-target effects that act on the ERK pathway (45). We therefore used a sub-clinical infection model to test for inflammatory phenotypes in the LRRK2 -/- mice. Mice were infected with *Salmonella typhimurium* and this revealed that LRRK2 significantly dampens the inflammatory response. In this model IL-18 comes most likely from myeloid cells, particularly monocytes and the principal inflammatory activator of *Salmonella* is LPS. This suggests that the observed differences in gene expression reported here cause subtle but significant changes in the inflammatory response in vivo that may be caused by alterations in the chemotactic capacity of monocytes and macrophages

It is interesting that only a small number of differentially expressed genes were observed between LRRK2 genotypes under resting conditions. This shows that LRRK2 only exerts an effect on the macrophage transcriptome under stimulated conditions. This finding also reflects work by another group that identified no changes in gene expression in unstimulated human fibroblasts or brain tissue between G2019S LRRK2 carriers and controls (46).

In conclusion the current study identifies the control of directional motility and chemotaxis of macrophages by LRRK2 as a potentially critical mechanism in the aetiology of PD. It suggests that the function and regulation of the LRRK2/EPAC-1/Rap1 axis and how this impacts on pro- and anti-inflammatory properties of microglia should be investigated. If active EPAC-1/Rap1 confers a neuroprotective phenotype on microglia, EPAC-1 specific agonists such as cAMP analog, 8-(4-chloro-phenylthio)-2′-O-methyladenosine-3′,5′-cyclic monophosphate (8-pCPT-2′-O-MecAMP) may have therapeutic value in PD (47).

Experimental procedures

Mice, genotyping and cell culture

WT C57BL/6J mice were obtained from Charles River, UK. LRRK2$^{-/-}$ B6.129X1(FVB)-Lrrk2$^{tm1.1Cai}$/J mice were obtained from The Jackson Laboratory, United States (48). All mice strains were bred independently. All work involving live animals complied with the University of Cambridge Ethics Committee regulations and was performed under the Home Office Project License number 80/2572. DNA from Ear snips of LRRK2$^{-/-}$ B6.129X1(FVB)-Lrrk2$^{tm1.1Cai}$/J mice was isolated for genotyping using the Phire animal tissue digest PCR kit (Thermo Fisher Scientific, USA). Genotyping PCR was carried out in accordance with recommendations by the Jackson Laboratory.. Genotyping PCR products were run on a 1 % agarose gel.

For the differentiation and culture of 'primary bone marrow derived macrophages' (pBMDMs), mice were killed between 8 and 16 weeks of age by cervical dislocation, skin was sterilized with 70 % ethanol, and legs removed. Under sterile conditions, the tibia and femur were isolated, cleaned of muscle, and the proximal and distal epiphysis cut away. Bone marrow was flushed out of the bone using primary growth media (Dulbecco's modified Eagle's medium (DMEM) (Thermo Fisher Scientific, USA) supplemented with 10 % foetal calf serum' (FCS) (Thermo Fisher Scientific, USA), 20 % L929 conditioned media and 8 mM L-glutamine (Sigma-Aldrich, USA)). Isolated cells were centrifuged at 300 *g* for 10 min at 15 °C, and re-suspended in 60 ml of growth media, and allowed to grow at 37 °C in 5 % CO_2. Cells were supplemented with a further 60 ml of growth media after 2 days, and media replaced every 3 days. All experiments were performed on cells between 6 and 11 days after initial bone marrow isolation. Live cell counts were performed using a haemocytometer with trypan blue staining (Sigma Aldrich, USA).

Animal Infections and Data Collection
S. Typhimurium strain M525P (49) a strain of intermediate virulence, was used to establish a subclinical infection in vivo. In particular, overnight (stationary phase) bacterial cultures were first washed and resuspended in Dulbecco's PBS (D-PBS, Sigma) and then diluted to the desired dose. Wild-type and Lrrk2-/- mice were subsequently challenged intravenously with 0.2ml of the bacterial suspension. The exact dose, as determined by serial dilution and plating the inoculum on LB plates before and after infection, was $1.3x10^4$ CFU/mouse. Mice were bled and then euthanised at certain intervals after the initial challenge, their spleens were aseptically removed and weighed. Mouse serum was analysed via ELISA for levels of IL-18 (MBL International) and IFN-γ (DuoSet Development kit, R&D Systems).

Flow cytometry
$1x10^6$ cells/well were plated in 12-well tissue culture plates and left to adhere over night at 37 °C in 5 % CO_2. Cells were then resuspended into MACS buffer (PBS supplemented with 2 % FCS, 1 mM EDTA (Merck and Co, USA)) and spun at 300 *g* for 6 minutes in a conical-bottom 96-well plate (Thermo Fisher Scientific, USA). To block Fc-mediated reactions, cells were re-suspended in MACS buffer supplemented with 1:100 rat anti-mouse CD16/CD32 functional grade purified (93 clone; eBioscience, USA) and incubated at 4 °C for 15 minutes. Cells were spun at 300 *g* for 6 minutes, then re-suspended in MACS buffer supplemented with rat anti-F4/80 conjugated with FITC, hamster anti-CD11c conjugated with phycoerythrin and rat anti-CD11b conjugated with PerCP-cyanine5.5. Staining was performed for 30 mins at 4 °C. Cells were then centrifuged at 300 *g* for 6 mins and re-suspended in MACS buffer 3 x to remove unbound antibody before finally being spun at 300 *g* for 6 minutes, and re-suspended in MACS buffer supplemented with 2 % methanol-free formaldehyde (Thermo Fisher Scientific, USA) to fix. Fixed cells were analysed using an Attune NxT acoustic focusing cytometer (Life Technologies, USA) for triple labeling experiments.

RNA sequencing and transcriptomic data analysis
Bone marrow was isolated from 16-week old female mice housed in the same facility for this study. $3x10^6$ cells/well were plated in Greiner 6-well tissue culture plates (Sigma-Aldrich, USA) a day prior to RNA extraction and left to adhere over night at 37 °C in 5 % CO_2. Where appropriate, cells were then treated with 100 ng/ml ultrapure LPS from *E. coli* O111:B4, or 10 µg/ml MDP. LPS was sonicated prior to application to cells. After 2 hours incubation at 37 °C in 5 % CO_2, cells were washed in PBS, then scraped into PBS at 4 °C. RNA was isolated using RNeasy mini kit in combination with QIAshredder cell homogenization following the manufacturers instructions. To remove genomic DNA, extracted RNA was DNase treated using TURBO DNA-free kit. Resulting RNA was analysed using a Nanodrop 1000 spectrophotometer. Samples with $A^{260/230} < 1.8$ were further purified with RNeasy MinElute Cleanup Kit (Qiagen, Germany). Samples were then flash frozen in liquid nitrogen, and RNA was quantified using a Qubit Fluorometer (Thermo Fisher Scientific, USA). RNA integrity was verified using 2100 Bioanlyser (Agilent Genomics, USA), and mRNA library preparation was performed using TruSeq Stranded mRNA Library Prep Kit (Illumina, USA) with quality control by 2200 Tapestation (Agilent Genomics, USA). High output sequencing runs of single-end 75 bp read length were performed on NextSeq500 (Illumina, USA) using NextSeq 500/550 High Output v2 Kit (75 cycles) (Illumina, USA). A minimum read depth of $18x10^6$ reads per sample was achieved. Read pre-processing, mapping with quality control was performed using a standard pipeline. Ensembl Mus_musculus.GRCm38.dna.primary_assembly .fa (release 84) reference genome file was used to map reads, using the annotated transcripts from the ensembl Mus_musculus.GRCm38.84.gtf. Differential gene expression analysis was performed using DESeq2. Analysis was performed as a 'paired comparison experiment' for each treatment group as comparisons between genotype are made between different samples of different mice (unpaired), while comparisons of treated vs untreated samples are made using samples from the same mice (paired). A target frame and design matrix were adapted from an analogous scenario laid out in the EdgeR user guide section 3.5: "Comparisons both between

and within subjects" (21). This analysis enabled simple differential gene expression analysis between genotypes, and 2-parameter analysis to compare responses of each genotype to innate immune stimuli by interrogation of a targets frame. This targets frame identifies each sample as belonging to a mouse (mouse.n), and each of these mice as being treated with LPS, MDP, or left untreated (media).

Quantitative reverse transcription PCR

qRT-PCR was performed using SensiFAST SYBR No-ROX One-Step Kit (Bioline, UK) following the manufacturers instructions and appropriate primers selected based on data submitted to the primer bank database (table 4)(50). qRT-PCR reactions were performed using a Rotor-Gene Q (Qiagen, Germany), and quantification of fold-changes of transcript were calculated using cycle threshold values accounting for reaction efficiency (51). For inhibitor studies, cells were pre-treated with 1.3 µM of GSK2578215A for four hours. Following this, they were treated with 100 ng/ml of LPS for a further two hours. Cells were then washed with 1X PBS and harvested. Total RNA was used for RT-qPCR using the Luna One step RT-qPCR kit (NEB) following the manufacturer's protocol.

Immunofluorescence microscopy

Cells were fixed with 4% paraformaldehyde and permeabilized with 0.1% Triton X100 (20min), and then blocked by washing with 0.05% Tween 20 in PBS, followed by blocking for 30min at 37ºC in 0.05% Tween 20 0.5% BSA. Cells were immune-stained overnight at 4ºC with Alexa-488 conjugated Anti-EPAC1 monoclonal antibody (Abcam ab201506). The Anti-Epac1 antibody is raised against human-EPAC but to an epitope that is conserved in the mouse homologue. After staining, slides were washed with blocking buffer, PBS, and then mounted in curing mountant with DAPI (Diamond antifade, Thermo Fisher P36966).

Fluorescence was detected under a FV1200 confocal microscope 60x oil immersion objective with integration as 512x512 pixels each 0.413x0.413µm with detector gain set for minimal saturated pixel count (4096 in the 13bit intensity Olympus format). Z-stacks of 5x1µm depth were collected upwards from the coverslip to collect the total cellular fluorescence. Projections summing each pixel in each z series were calculated in ImageJ and the image converted to 'FITS' image format to preserve the Olympus raw pixel intensity count data. Fields of view from media-treated and LPS-treated cells for each genotype were collected in batches of 10 images as close in time as possible. As a result intensity differences within a genotype are more reliable than comparison between genotypes. This approach was chosen so that the differing response of the cell types to LPS could be detected more accurately.

Projection image analysis was with Mathematica 11 – cell bodies were masked using the MorphologicalBinarize function extended by a border of 5 pixels (2µm) for edge inclusion. Cell number was obtained from the binarized DAPI channel using the MorphologicalComponent function to give a count of the nuclei. EPAC1 immuno-fluorescence from both cytoplasm and nuclei compartments were summed typically giving an intensity of millions of Olympus fluorescence units. Data from approximately 200-300 cells in 20 fields of view were analysed for each sample and reported mean intensity given in million units per cell. Cells cut by image borders were included in the pixel counts even if not containing the nucleus (as on average a cell should be cut by a border into two halves one with and one without a nucleus). The mean total intensity per cell was calculated as a measure of EPAC1 expression with a S.E.M. based on number of fields of view included (rather than the number of cells). Ratios of average fluorescence per cell in LPS treated vs medium were calculated at each time point for each genotype. In addition, the ratio of wild-type to knockout cells was calculated.

Acknowledgements: We would like to thank the Cambridge Genomic Services for RNA sequencing.

Conflict of interest: The authors declare that they have no conflicts of interest with the contents of this article

Author contributions (CRediT Terms): Conceptualization DL, NJG, CEB; Investigation, Formal Analysis, Writing-Original Draft, Preparation and Visualization DL, NJG, CEB, MFS, LJH, PT; Validation MFS, DL; Resources CEB, NJG,; Writing-Review & Editing, NJG and DL; Supervision CEB and NJG.

References

1. Mills, R. D., T. D. Mulhern, F. Liu, J. G. Culvenor, and H. C. Cheng. 2014. Prediction of the repeat domain structures and impact of parkinsonism-associated variations on structure and function of all functional domains of leucine-rich repeat kinase 2 (LRRK2). *Hum Mutat* 35: 395-412.
2. Marin, I., W. N. van Egmond, and P. J. van Haastert. 2008. The Roco protein family: a functional perspective. *FASEB J* 22: 3103-3110.
3. Russo, I., G. Berti, N. Plotegher, G. Bernardo, R. Filograna, L. Bubacco, and E. Greggio. 2015. Leucine-rich repeat kinase 2 positively regulates inflammation and down-regulates NF-kappaB p50 signaling in cultured microglia cells. *J Neuroinflammation* 12: 230.
4. Di Fonzo, A., C. F. Rohe, J. Ferreira, H. F. Chien, L. Vacca, F. Stocchi, L. Guedes, E. Fabrizio, M. Manfredi, N. Vanacore, S. Goldwurm, G. Breedveld, C. Sampaio, G. Meco, E. Barbosa, B. A. Oostra, V. Bonifati, and N. Italian Parkinson Genetics. 2005. A frequent LRRK2 gene mutation associated with autosomal dominant Parkinson's disease. *Lancet* 365: 412-415.
5. Nichols, W. C., N. Pankratz, D. Hernandez, C. Paisan-Ruiz, S. Jain, C. A. Halter, V. E. Michaels, T. Reed, A. Rudolph, C. W. Shults, A. Singleton, T. Foroud, and P. i. Parkinson Study Group. 2005. Genetic screening for a single common LRRK2 mutation in familial Parkinson's disease. *Lancet* 365: 410-412.
6. Gilks, W. P., P. M. Abou-Sleiman, S. Gandhi, S. Jain, A. Singleton, A. J. Lees, K. Shaw, K. P. Bhatia, V. Bonifati, N. P. Quinn, J. Lynch, D. G. Healy, J. L. Holton, T. Revesz, and N. W. Wood. 2005. A common LRRK2 mutation in idiopathic Parkinson's disease. *Lancet* 365: 415-416.
7. Greggio, E., L. Civiero, M. Bisaglia, and L. Bubacco. 2012. Parkinson's disease and immune system: is the culprit LRRKing in the periphery? *J Neuroinflammation* 9: 94.
8. Gardet, A., Y. Benita, C. Li, B. E. Sands, I. Ballester, C. Stevens, J. R. Korzenik, J. D. Rioux, M. J. Daly, R. J. Xavier, and D. K. Podolsky. 2010. LRRK2 is involved in the IFN-gamma response and host response to pathogens. *J Immunol* 185: 5577-5585.
9. Thevenet, J., R. Pescini Gobert, R. Hooft van Huijsduijnen, C. Wiessner, and Y. J. Sagot. 2011. Regulation of LRRK2 expression points to a functional role in human monocyte maturation. *PLoS One* 6: e21519.
10. Dzamko, N., F. Inesta-Vaquera, J. Zhang, C. Xie, H. Cai, S. Arthur, L. Tan, H. Choi, N. Gray, P. Cohen, P. Pedrioli, K. Clark, and D. R. Alessi. 2012. The IkappaB kinase family phosphorylates the Parkinson's disease kinase LRRK2 at Ser935 and Ser910 during Toll-like receptor signaling. *PLoS One* 7: e39132.
11. Karin, M. 1999. How NF-kappaB is activated: the role of the IkappaB kinase (IKK) complex. *Oncogene* 18: 6867-6874.
12. Castano, A., A. J. Herrera, J. Cano, and A. Machado. 2002. The degenerative effect of a single intranigral injection of LPS on the dopaminergic system is prevented by dexamethasone, and not mimicked by rh-TNF-alpha, IL-1beta and IFN-gamma. *J Neurochem* 81: 150-157.
13. Iravani, M. M., C. C. Leung, M. Sadeghian, C. O. Haddon, S. Rose, and P. Jenner. 2005. The acute and the long-term effects of nigral lipopolysaccharide administration on dopaminergic dysfunction and glial cell activation. *Eur J Neurosci* 22: 317-330.
14. Qin, L., X. Wu, M. L. Block, Y. Liu, G. R. Breese, J. S. Hong, D. J. Knapp, and F. T. Crews. 2007. Systemic LPS causes chronic neuroinflammation and progressive neurodegeneration. *Glia* 55: 453-462.
15. Niehaus, I., and J. H. Lange. 2003. Endotoxin: is it an environmental factor in the cause of Parkinson's disease? *Occup Environ Med* 60: 378.
16. Jang, H., D. A. Boltz, R. G. Webster, and R. J. Smeyne. 2009. Viral parkinsonism. *Biochim Biophys Acta* 1792: 714-721.
17. Murray, P. J., and T. A. Wynn. 2011. Protective and pathogenic functions of macrophage subsets. *Nat Rev Immunol* 11: 723-737.

18. Love, M. I., W. Huber, and S. Anders. 2014. Moderated estimation of fold change and dispersion for RNA-seq data with DESeq2. *Genome Biol* 15: 550.
19. Linde, L., S. Boelz, G. Neu-Yilik, A. E. Kulozik, and B. Kerem. 2007. The efficiency of nonsense-mediated mRNA decay is an inherent character and varies among different cells. *Eur J Hum Genet* 15: 1156-1162.
20. Akagi, K., J. Li, R. M. Stephens, N. Volfovsky, and D. E. Symer. 2008. Extensive variation between inbred mouse strains due to endogenous L1 retrotransposition. *Genome Res* 18: 869-880.
21. Robinson, M. D., D. J. McCarthy, and G. K. Smyth. 2010. edgeR: a Bioconductor package for differential expression analysis of digital gene expression data. *Bioinformatics* 26: 139-140.
22. Reith, A. D., P. Bamborough, K. Jandu, D. Andreotti, L. Mensah, P. Dossang, H. G. Choi, X. Deng, J. Zhang, D. R. Alessi, and N. S. Gray. 2012. GSK2578215A; a potent and highly selective 2-arylmethyloxy-5-substitutent-N-arylbenzamide LRRK2 kinase inhibitor. *Bioorg Med Chem Lett* 22: 5625-5629.
23. Robichaux, W. G., 3rd, and X. Cheng. 2018. Intracellular cAMP Sensor EPAC: Physiology, Pathophysiology, and Therapeutics Development. *Physiol Rev* 98: 919-1053.
24. Lorenowicz, M. J., J. van Gils, M. de Boer, P. L. Hordijk, and M. Fernandez-Borja. 2006. Epac1-Rap1 signaling regulates monocyte adhesion and chemotaxis. *J Leukoc Biol* 80: 1542-1552.
25. Yi, L., P. Chandrasekaran, and S. Venkatesan. 2012. TLR signaling paralyzes monocyte chemotaxis through synergized effects of p38 MAPK and global Rap-1 activation. *PLoS One* 7: e30404.
26. Choi, I., B. Kim, J. W. Byun, S. H. Baik, Y. H. Huh, J. H. Kim, I. Mook-Jung, W. K. Song, J. H. Shin, H. Seo, Y. H. Suh, I. Jou, S. M. Park, H. C. Kang, and E. H. Joe. 2015. LRRK2 G2019S mutation attenuates microglial motility by inhibiting focal adhesion kinase. *Nat Commun* 6: 8255.
27. Zlotnik, A., and O. Yoshie. 2000. Chemokines: a new classification system and their role in immunity. *Immunity* 12: 121-127.
28. Turner, M. D., B. Nedjai, T. Hurst, and D. J. Pennington. 2014. Cytokines and chemokines: At the crossroads of cell signalling and inflammatory disease. *Biochim Biophys Acta* 1843: 2563-2582.
29. Migeotte, I., J. D. Franssen, S. Goriely, F. Willems, and M. Parmentier. 2002. Distribution and regulation of expression of the putative human chemokine receptor HCR in leukocyte populations. *Eur J Immunol* 32: 494-501.
30. Yoshimura, T., and J. J. Oppenheim. 2011. Chemokine-like receptor 1 (CMKLR1) and chemokine (C-C motif) receptor-like 2 (CCRL2); two multifunctional receptors with unusual properties. *Exp Cell Res* 317: 674-684.
31. Akram, I. G., R. Georges, T. Hielscher, H. Adwan, and M. R. Berger. 2016. The chemokines CCR1 and CCRL2 have a role in colorectal cancer liver metastasis. *Tumour Biol* 37: 2461-2471.
32. Ma, B., L. Xu, X. Pan, L. Sun, J. Ding, C. Xie, V. E. Koliatsos, and H. Cai. 2016. LRRK2 modulates microglial activity through regulation of chemokine (C-X3-C) receptor 1 -mediated signalling pathways. *Hum Mol Genet* 25: 3515-3523.
33. Cascon, A., and M. Robledo. 2012. MAX and MYC: a heritable breakup. *Cancer Res* 72: 3119-3124.
34. Gilchrist, M., V. Thorsson, B. Li, A. G. Rust, M. Korb, J. C. Roach, K. Kennedy, T. Hai, H. Bolouri, and A. Aderem. 2006. Systems biology approaches identify ATF3 as a negative regulator of Toll-like receptor 4. *Nature* 441: 173-178.
35. Liu, H., D. C. Radisky, D. Yang, R. Xu, E. S. Radisky, M. J. Bissell, and J. M. Bishop. 2012. MYC suppresses cancer metastasis by direct transcriptional silencing of alphav and beta3 integrin subunits. *Nat Cell Biol* 14: 567-574.
36. Ishiguro, H., T. Tsunoda, T. Tanaka, Y. Fujii, Y. Nakamura, and Y. Furukawa. 2001. Identification of AXUD1, a novel human gene induced by AXIN1 and its reduced expression in human carcinomas of the lung, liver, colon and kidney. *Oncogene* 20: 5062-5066.
37. Gingras, S., S. Pelletier, K. Boyd, and J. N. Ihle. 2007. Characterization of a family of novel cysteine-serine-rich nuclear proteins (CSRNP). *PLoS One* 2: e808.
38. Nakamura, T., F. Hamada, T. Ishidate, K. Anai, K. Kawahara, K. Toyoshima, and T. Akiyama. 1998. Axin, an inhibitor of the Wnt signalling pathway, interacts with beta-catenin, GSK-3beta and APC and reduces the beta-catenin level. *Genes Cells* 3: 395-403.
39. Roy, A., S. B. Rangasamy, M. Kundu, and K. Pahan. 2016. BPOZ-2 Gene Delivery Ameliorates Alpha-Synucleinopathy in A53T Transgenic Mouse Model of Parkinson's Disease. *Sci Rep* 6: 22067.
40. Wakade, C., and R. Chong. 2014. A novel treatment target for Parkinson's disease. *J Neurol Sci* 347: 34-38.
41. Wakade, C., R. Chong, E. Bradley, B. Thomas, and J. Morgan. 2014. Upregulation of GPR109A in Parkinson's disease. *PLoS One* 9: e109818.

42. Lukasova, M., J. Hanson, S. Tunaru, and S. Offermanns. 2011. Nicotinic acid (niacin): new lipid-independent mechanisms of action and therapeutic potentials. *Trends Pharmacol Sci* 32: 700-707.
43. Digby, J. E., F. Martinez, A. Jefferson, N. Ruparelia, J. Chai, M. Wamil, D. R. Greaves, and R. P. Choudhury. 2012. Anti-inflammatory effects of nicotinic acid in human monocytes are mediated by GPR109A dependent mechanisms. *Arterioscler Thromb Vasc Biol* 32: 669-676.
44. Zandi-Nejad, K., A. Takakura, M. Jurewicz, A. K. Chandraker, S. Offermanns, D. Mount, and R. Abdi. 2013. The role of HCA2 (GPR109A) in regulating macrophage function. *FASEB J* 27: 4366-4374.
45. Luerman, G. C., C. Nguyen, H. Samaroo, P. Loos, H. Xi, A. Hurtado-Lorenzo, E. Needle, G. Stephen Noell, P. Galatsis, J. Dunlop, K. F. Geoghegan, and W. D. Hirst. 2014. Phosphoproteomic evaluation of pharmacological inhibition of leucine-rich repeat kinase 2 reveals significant off-target effects of LRRK-2-IN-1. *J Neurochem* 128: 561-576.
46. Devine, M. J., A. Kaganovich, M. Ryten, A. Mamais, D. Trabzuni, C. Manzoni, P. McGoldrick, D. Chan, A. Dillman, J. Zerle, S. Horan, J. W. Taanman, J. Hardy, J. F. Marti-Masso, D. Healy, A. H. Schapira, B. Wolozin, R. Bandopadhyay, M. R. Cookson, M. P. van der Brug, and P. A. Lewis. 2011. Pathogenic LRRK2 mutations do not alter gene expression in cell model systems or human brain tissue. *PLoS One* 6: e22489.
47. Banerjee, U., and X. Cheng. 2015. Exchange protein directly activated by cAMP encoded by the mammalian rapgef3 gene: Structure, function and therapeutics. *Gene* 570: 157-167.
48. Parisiadou, L., C. Xie, H. J. Cho, X. Lin, X. L. Gu, C. X. Long, E. Lobbestael, V. Baekelandt, J. M. Taymans, L. Sun, and H. Cai. 2009. Phosphorylation of ezrin/radixin/moesin proteins by LRRK2 promotes the rearrangement of actin cytoskeleton in neuronal morphogenesis. *J Neurosci* 29: 13971-13980.
49. Mastroeni, P., A. Vazquez-Torres, F. C. Fang, Y. Xu, S. Khan, C. E. Hormaeche, and G. Dougan. 2000. Antimicrobial actions of the NADPH phagocyte oxidase and inducible nitric oxide synthase in experimental salmonellosis. II. Effects on microbial proliferation and host survival in vivo. *J Exp Med* 192: 237-248.
50. Spandidos, A., X. Wang, H. Wang, and B. Seed. 2010. PrimerBank: a resource of human and mouse PCR primer pairs for gene expression detection and quantification. *Nucleic Acids Res* 38: D792-799.
51. Pfaffl, M. W. 2001. A new mathematical model for relative quantification in real-time RT-PCR. *Nucleic Acids Res* 29: e45.

FOOTNOTES

This work was funded by Wellcome Trust Investigator awards (WT100321/z/12/Z and 108045/Z/15/Z) to CEB and NJG. DL was supported by a Wellcome Trust Infection and Immunity studentship.

The abbreviations used are: PD, Parkinson's disease; LRRK2, leucine rich repeat kinase 2; CCL, chemokine ligand; GWAS, genome wide association studies; LPS, lipopolysaccharide; MDP, muramyl dipeptide; EPAC, exchange factor directly activated by cAMP; NF*k*B, nuclear factor kappa B; qRT-PCR, quantitative reverse transcription polymerase chain reaction.

Ensembl gene ID	baseMean	Fold change (KO/WT)	Padj	Gene Symbol
ENSMUSG00000082809	177.98	5.65	2.52E-92	Pseudogene Gm14150
ENSMUSG00000063458	83.02	0.44	3.99E-20	Lrmda
ENSMUSG00000022629	31.47	1.93	1.07E-14	Kif21a
ENSMUSG00000105703	89.25	2.01	1.94E-13	Gm43305
ENSMUSG00000036273	137.37	0.54	8.10E-10	Lrrk2
ENSMUSG00000057897	58.28	1.66	1.17E-07	Camk2b
ENSMUSG00000032679	297.27	1.55	1.02E-04	Cd59a
ENSMUSG00000025453	784.61	1.43	9.56E-04	Nnt

Table 1: Differentially expressed genes between unstimulated macrophages. Genes with padj < 0.01. LRRK2 KO/WT pBMDM cells. Genes not represented at the protein level are displayed in grey.

Ensembl gene ID	baseMean	Fold change (KO/WT)	Padj	Gene Symbol
ENSMUSG00000022469	176.34	10.97	4.98E-37	Rapgef3
ENSMUSG00000018930	11796.25	3.26	1.94E-12	Ccl4
ENSMUSG00000026628	2039.03	2.72	5.58E-07	Atf3
ENSMUSG00000000982	4095.93	2.24	1.02E-03	Ccl3
ENSMUSG00000032515	1117.61	1.73	1.07E-03	Csrnp1
ENSMUSG00000032724	417.68	2.80	5.72E-03	Abtb2
ENSMUSG00000035042	3664.77	2.02	2.75E-02	Ccl5
ENSMUSG00000043953	1652.79	3.39	2.75E-02	Ccrl2
ENSMUSG00000045502	249.85	3.55	4.19E-02	Hcar2
ENSMUSG00000001156	477.83	2.09	9.07E-02	Mxd1
ENSMUSG00000000275	8075.68	1.40	9.83E-02	Trim25

Table 2: Differentially responding genes in LPS stimulated macrophages. Genes with padj < 0.1. LPS treated LRRK2 KO/WT pBMDM cells.

a

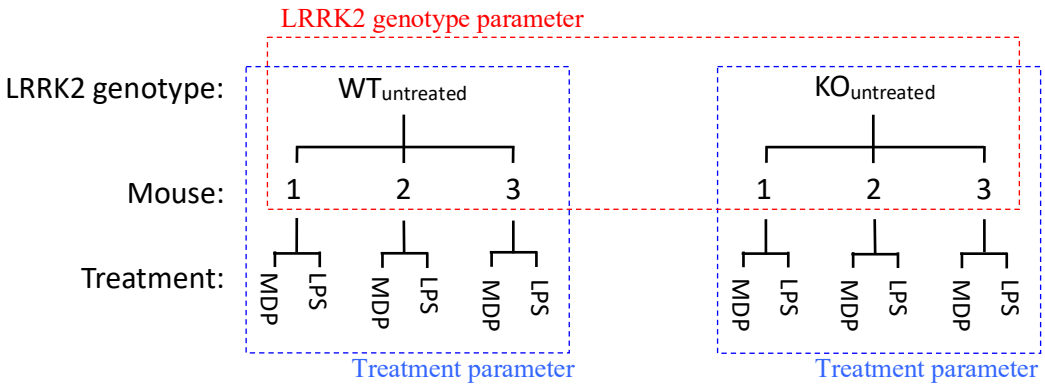

b

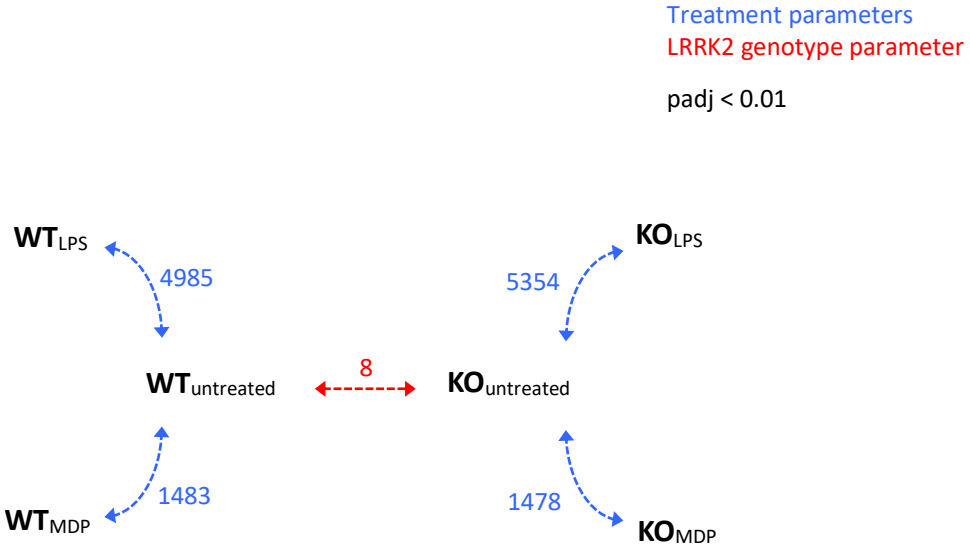

Figure 1: Differential gene expression analysis. a: LRRK2 genotype (red), and treatment with innate immune stimuli (blue), are considered separately in these experiments. **b**: Quantification of differentially expressed genes. KO refers to the LRRK2 KO genotype. Numbers refer to differentially expressed genes between annotated samples (padj < 0.01).

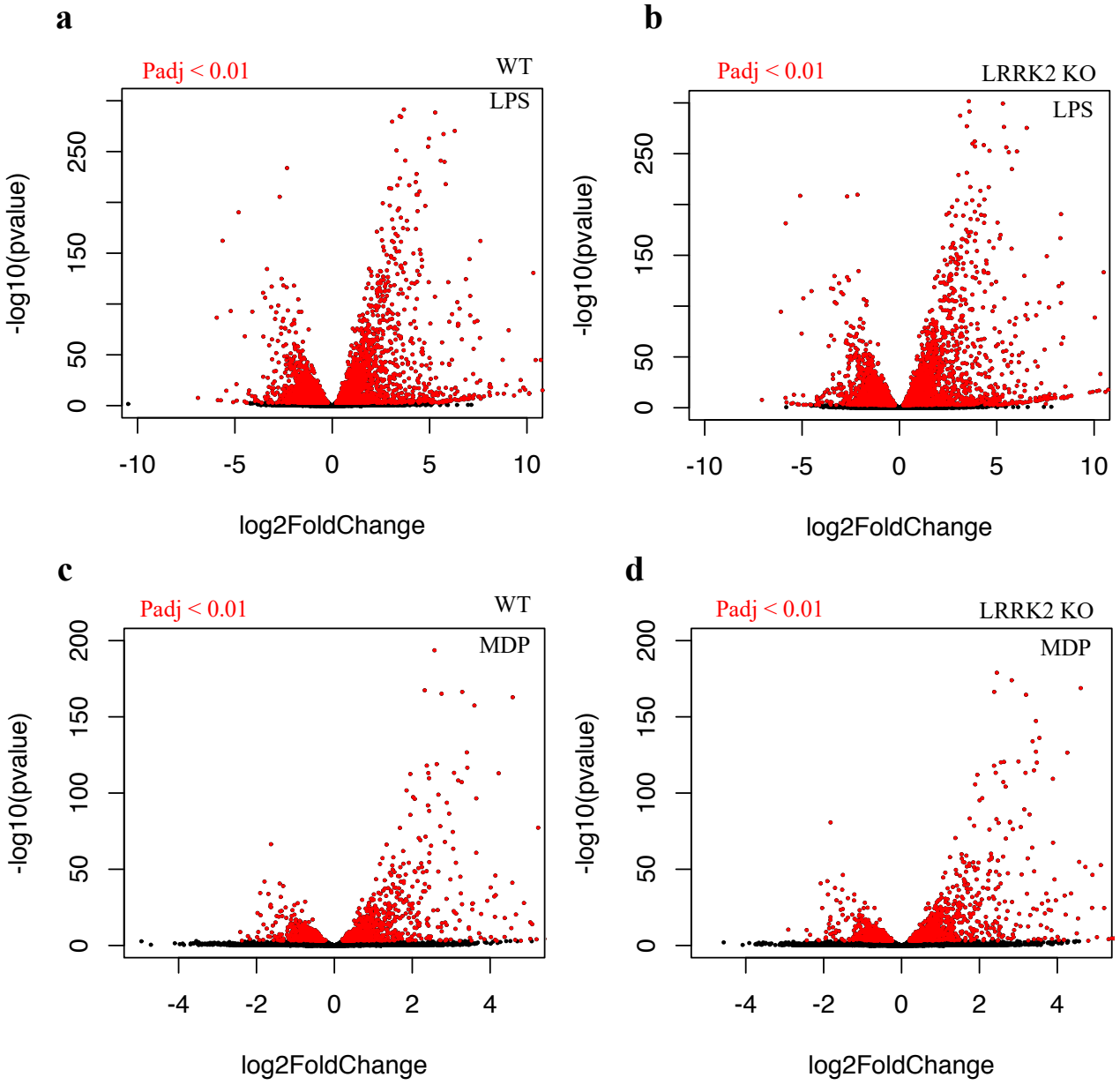

Figure 2: 'Volcano plot' visualisation of transcriptional gene responses. Dots represent individual genes. Red indicates padj < 0.01. **a,c:** WT pBMDM cells. **b,d:** LRRK2 KO pBMDM cells.

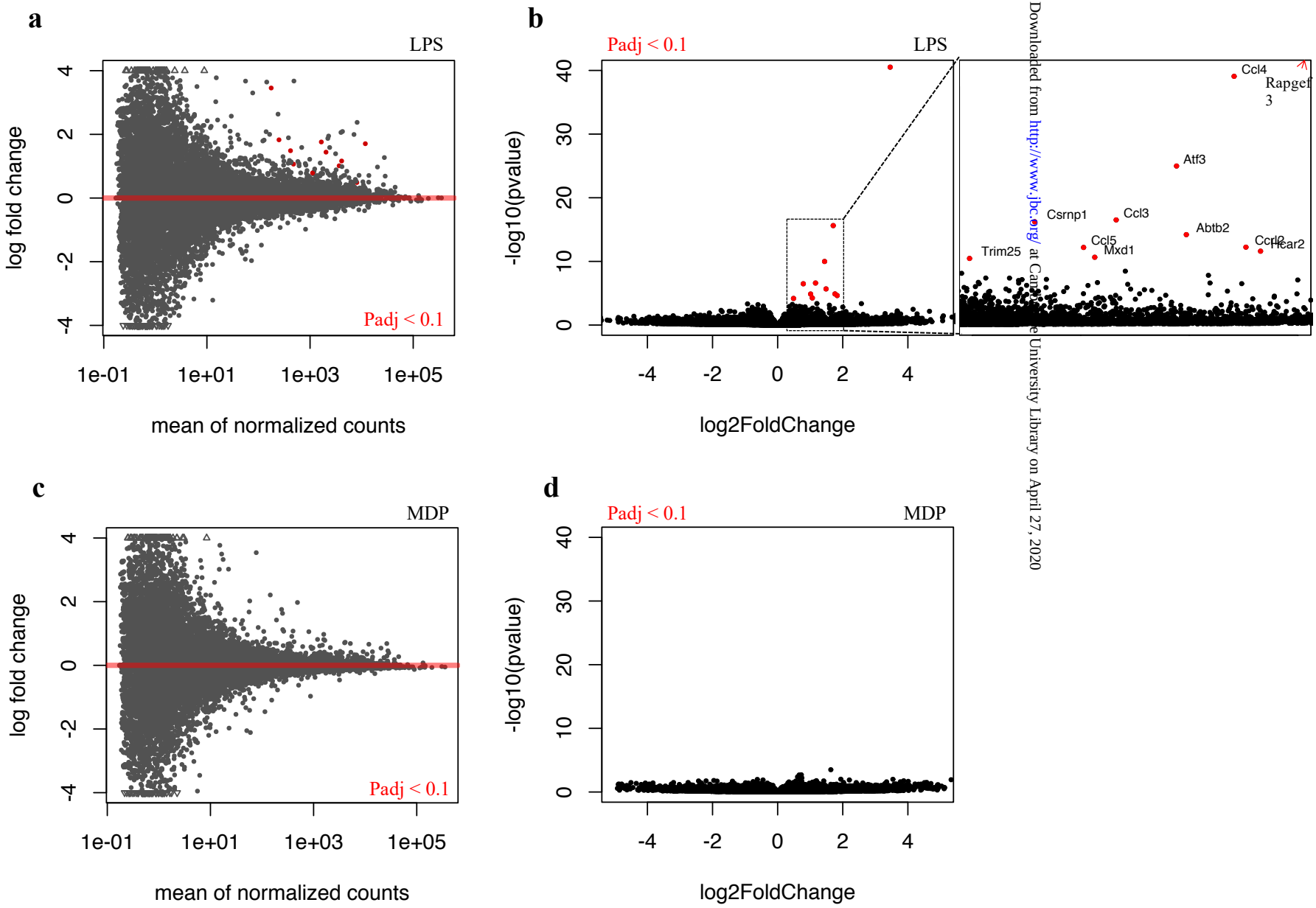

Figure 3: Visualisation of differentially responding genes. Fold changes are ligand treated gene expression levels (LRRK2 KO/WT). Dots represent individual genes. Red dots indicate padj < 0.1

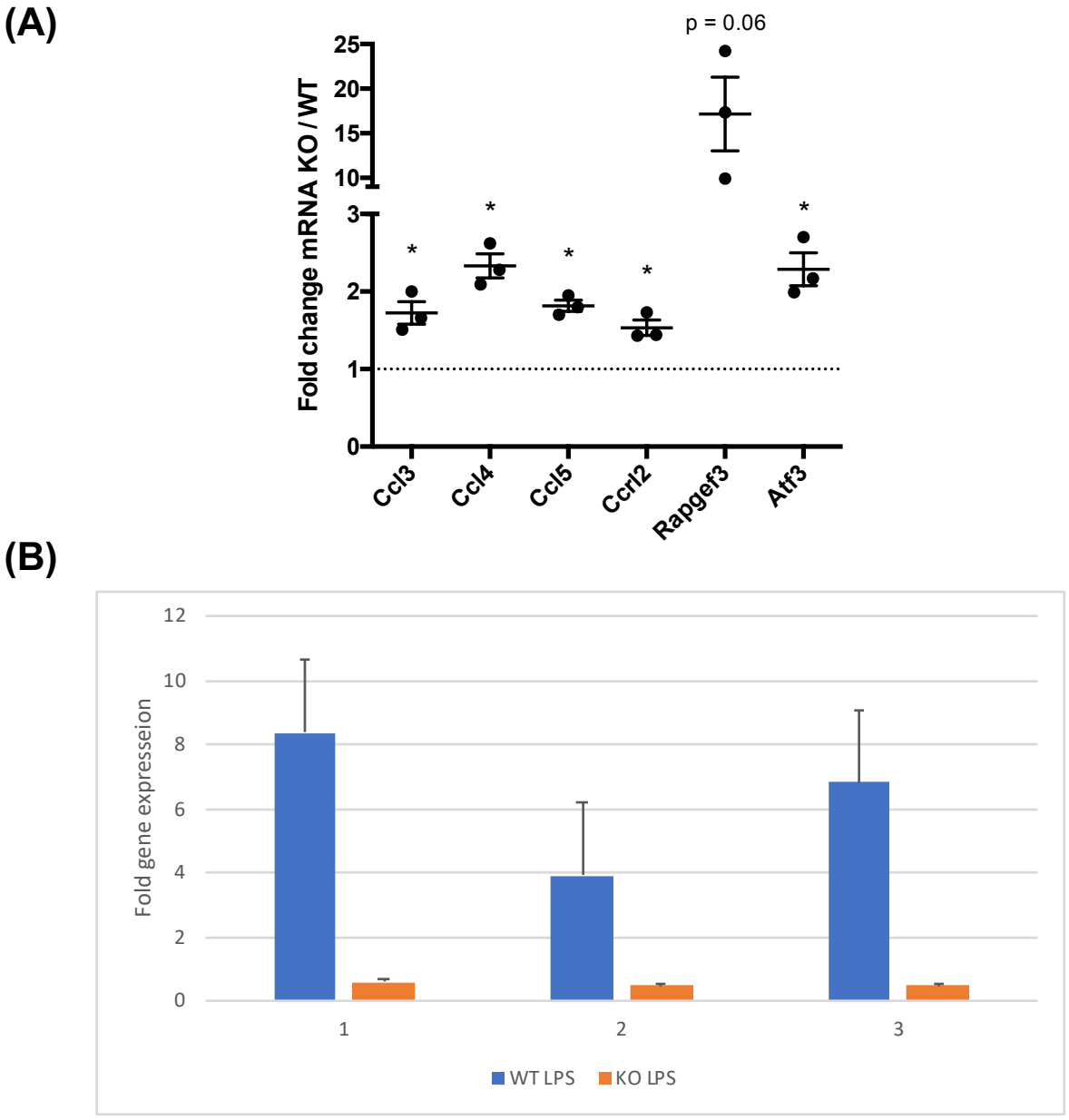

Figure 4: Transcript levels upon LPS stimulation. (A) qRT-PCR with beta-actin and GAPDH as housekeeping genes. Each point is a different LRRK2 KO pBMDM sample compared to three different WT pBMDM samples. Error bars are S.E.M. Paired two-tailed t tests compared to a value of 1. (B) Equal aliquots of wild type (blue bars) and LRRK2 -/- (orange bars) macrophages were incubated for 4 hours with or without the GSK2578215A inhibitor (1.3µM) and then stimulated with LPS for 2 hours. *Rapgef3* RNA was then quantified by qRT-PCR. Wild type, untreated cells have active LRRK2 and therefore *Rapgef3* expression is relatively inhibited as compared to the equivalent treated cells whereas mutant macrophages have similar levels of *Rapgef3* transcript in treated and control samples. Results are presented for three biological replicates.

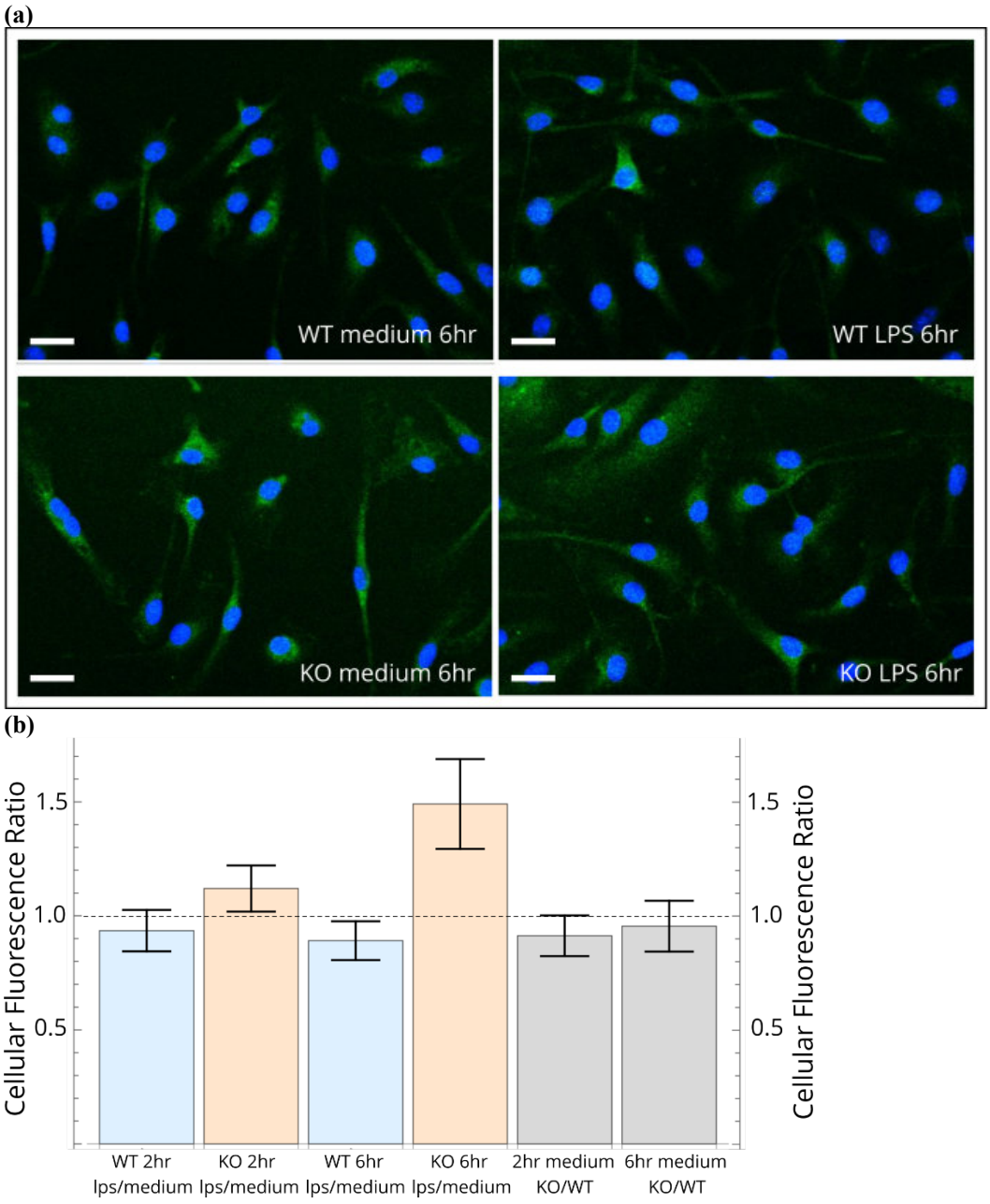

Figure 5. Elevated levels of EPAC-1 in activated macrophages lacking LRRK2.
(a) Immunofluorescent images of cells stained with Alexa-488 conjugated Anti-EPAC1 monoclonal antibody (green) and DAPI (blue).
(b) Projection image analysis of untreated and LPS stimulated macrophages. The ratios of average fluorescence per cell in LPS treated vs medium were calculated at each time point for each genotype (see methods). Scale bar is 20μM.

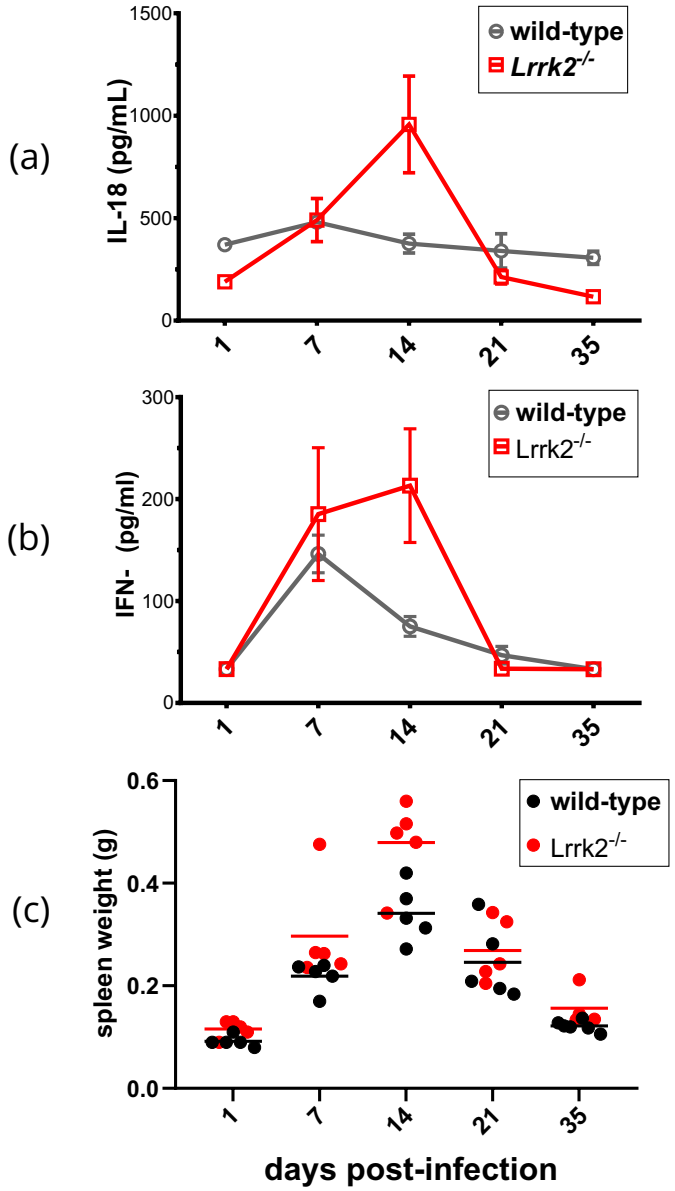

Figure 6. LRRK2 dampens inflammation in a subclinical infection model.
Wildtype and LRRK2 -/- (n=5) mice were infected with *Salmonella typhimurium* 525P. IL-18 (a), interferon γ (b) and spleen weight (c) were measured. Significance was evaluated with the Man-Whitney test. Differences in IL-18 were significant (day1: P=0.0159 (*), day 14: P=0.0159 (*) day 35: P=0.0095 (**)), IFNγ although elevated at day 14 was not significant at the 95% confidence level (p= 0.09), spleen weight was significant at day 14: P=0.0317 (*).

Parkinson's disease–associated kinase LRRK2 regulates genes required for cell adhesion, polarization, and chemotaxis in activated murine macrophages

Daniel R Levy, Atul Udgata, Panagiotis Tourlomousis, Martyn F Symmons, Lee J Hopkins, Clare E Bryant and Nicholas J. Gay

J. Biol. Chem. published online February 28, 2020
